

1993

Lumped and distributed models for long bond wires

Yevgeniy A. Tkachenko
Lehigh University

Follow this and additional works at: <http://preserve.lehigh.edu/etd>

Recommended Citation

Tkachenko, Yevgeniy A., "Lumped and distributed models for long bond wires" (1993). *Theses and Dissertations*. Paper 183.

This Thesis is brought to you for free and open access by Lehigh Preserve. It has been accepted for inclusion in Theses and Dissertations by an authorized administrator of Lehigh Preserve. For more information, please contact preserve@lehigh.edu.

AUTHOR:

Tkachenko, Yevgeniy A.

TITLE:

**Lumped and Distributed
Models for Long Bond
Wires**

DATE: May 30, 1993

**LUMPED AND DISTRIBUTED MODELS
FOR LONG BOND WIRES**

by

Yevgeniy A. Tkachenko

A Thesis

Presented to the Graduate Committee

of Lehigh University

in Candidacy for the Degree of

Master of Science

in

Electrical Engineering

Lehigh University

May 1993

This thesis is accepted and approved in partial fulfillment of the requirements for the
Master of Science in Electrical Engineering..

5/10/93
Date

Professor J.C.M. Hwang
Thesis Advisor

Chairman of Department

ACKNOWLEDGEMENTS

I would like to thank my advisor, Dr. James C.M. Hwang for his support and valuable suggestions, and people at Compound Semiconductor Technology Laboratory, specially Dave Whitefield and Dr. Cejun Wei for their continuous help in the lab.

I am addressing very special thanks to Liena and Elizabeth for being the greatest wife and daughter man could ever imagine. I extend my love and appreciation to my big family in Kiev, specially to my and Liena's parents for their tremendous encouragement. I am gratefully thankful to Mr. and Mrs. Taylor who made my graduate studies possible.

TABLE OF CONTENTS	PAGE
TITLE PAGE	i
CERTIFICAL OF APPROVAL	ii
ACKNOWLEDGEMENTS	iii
TABLE OF CONTENTS	iv
LIST OF TABLES	vi
LIST OF FIGURES	vii
ABSTRACT	1
1. INTRODUCTION	2
2. LUMPED AND DISTRIBUTED BOND WIRE MODELS	4
2.1 LUMPED INDUCTANCE MODEL	5
2.2 TRANSMISSION LINE MODEL	8
2.3 WIRE RESISTANCE AND PAD CAPACITANCE	9
3. PROPOSED MODEL EXTRACTION AND VERIFICATION	11
4. RESULTS AND DISCUSSION	13
4.1 LRC MODELING RESULTS	14
4.2 TRANSMISSION LINE MODELING RESULTS	15
4.3 EFFECT OF NON-SYMMETRICAL SHAPE	17
5. CONCLUSIONS	18
6. FUTURE WORK	19

BIBLIOGRAPHY	20
TABLES	21
FIGURES	23
VITA	43

List of Tables

Table 1. Extracted LRC model parameters

Table 2. Extracted transmission line model parameters

List of Figures

Figure 1. Schematic of a 10 W C-band amplifier

Figure 2. Lumped LRC model of a bond wire

Figure 3. Transmission line model of a bond wire

Figure 4. Schematic of a bond wire structure

Figure 5. Per unit length series resistance of wires 25 μm in diameter

Figure 6. Proposed bond wire modeling scheme

Figure 7. Modeled [2], em simulated and measured transmission coefficient S_{21} of a wire 0.65 mm high and 1.3 mm in span

Figure 8. Modeled [2], em simulated and measured reflection coefficient S_{11} of a wire 0.65 mm high and 1.3 mm in span

Figure 9. Bond wire measurement schematic

Figure 10. Extracted wire inductances as a function of wire span and height

Figure 11. Extracted wire inductances as a function of wire length only

Figure 12. Wire inductance calculated according to [1], [2], [3] and extracted values

Figure 13. Em simulated and modeled reflection coefficient S_{11} of wires with $a = 0.5$ mm, $b = 1$ mm and $a = 0.9$ mm, $b = 2$ mm

Figure 14. Em simulated and modeled transmission coefficient S_{21} of wires with $a = 0.5$ mm,

$b = 1 \text{ mm}$ and $a = 0.9 \text{ mm}$, $b = 2 \text{ mm}$

Figure 15. Simulated transmission coefficient S_{21} of wires 0.9 mm high and 1, 2, 3.2 and 4 mm in span.

Figure 16. Transmission coefficient S_{21} of a wire 0.9 mm high and 4 mm in span predicted by em simulation and LCR and transmission line models

Figure 17. Extracted effective transmission line lengths

Figure 18. Extracted effective dielectric constants

Figure 19. Symmetrical and non-symmetrical wire geometries used for simulation

Figure 20. Em simulated transmission coefficient S_{21} of symmetrical and non-symmetrical wires 0.5 mm high and 1 mm in span

Figure 21. Em simulated reflection coefficient S_{11} of symmetrical and non-symmetrical wires 0.5 mm high and 1 mm in span

ABSTRACT

Accurate and efficient models have been developed for long bond wires. Lumped elements model can be used up to 16 GHz for relatively short bond wires. Above 16 GHz a distributed transmission line model is required. Simple empirical expressions were derived for the major model parameters. Both models are conveniently incorporated within a commercial microwave integrated circuit simulator.

Chapter 1

Introduction

Gold bond wires are widely used in modern microwave integrated circuits (MICs). The wires are used to connect the circuit to the outside world and to form a part of the impedance matching networks. As the frequency of operation increases wire length approaches a fraction of wavelength and distributive properties come into play. If not properly treated, bond wires may perturb impedance matching and circuit operation in general. Thus, accurate characterization and modeling of bond wires is especially critical at high frequencies. An example of how important it is to model the bond wires is described in [11]. This paper reports a large-signal nonlinear model of a 10 Watt C-band packaged amplifier. The amplifier includes two 144-finger GaAs MESFET's and off-chip matching networks to provide power combining and tuning in the desired frequency range (Figure 1). Because of the large transistor size, the tuning capacitors should be connected to each 12-finger transistor unit cell with many rather long bond wires. It was experimentally found that power is distributed non-uniformly between different unit cells, therefore degrading amplifier output power and linearity. Partially nonuniform power distribution is attributed to different lengths of different bond wires, hence different series

inductance or characteristic impedance presented to the signal. Thus, accurate models for the bond wires are necessary to construct large-signal nonlinear model of the whole amplifier. Specially developed wire models described in this thesis made a certain contribution to the comprehensive model of the MESFET amplifier [11] that was proven to predict for the first time peculiar nonlinear behavior as well as the power performance of the circuit.

This work discusses in detail lumped and distributed approaches to model bond wires, summarizes previously reported methods of wire characterization and introduces new models based on the results of numerical 2.5-dimensional full-wave electromagnetic simulation.

Chapter 2

Lumped and distributed bond wire models

There are two basic approaches to model bond wires. The first approach is to use a series combination of wire inductance and parasitic resistance and at the ends connect two shunt capacitors representing fringe capacitances of the bonding pads. The schematic of an *LRC* wire model is shown in Figure 2. The incremental parallel wire capacitance is usually too small to be included in the model. The second approach is to represent the wire as a transmission line with its characteristic impedance and effective dielectric constant. Such a distributed model is shown schematically in Figure 3. The width of this transmission line corresponds to the wire diameter. In general the length of the transmission line is not equal to the actual wire length hence will be called "effective transmission line length" in the model proposed below.

The terms "*LRC* model" and "transmission line model" will be used interchangeably with "lumped model" and "distributed model", respectively.

2.1 LUMPED INDUCTANCE MODEL.

Equivalent wire inductance is the most critical element of the LRC model.

Different ways to calculate it were reported in literature.

The simplest way is to use the formula for the "free space" self-inductance of circular ring of round wire for nonmagnetic materials [1]:

$$L_1 = \frac{a}{100} [7.4 \log 32a/d - 6.4] \mu H \quad (1)$$

where a = mean radius of ring in inches, d = diameter of wire in inches. The geometry used in this and all other approaches are shown in Figure 4. Equation (1), however, is accurate only at ultra-high frequencies (UHF).

Another set of formulas of "free space" wire inductance were derived from the electromagnetic theory was proposed in [2]:

$$L_2 = \left(\frac{\mu_0 l}{2\pi}\right) \left[\ln\left(\frac{4l}{d}\right) + \frac{\mu_r}{4} - 1 \right] \quad (2)$$

$$L_3 = \left(\frac{\mu_0 l}{2\pi}\right) \left[\ln\left[\left(\frac{2l}{d}\right) + \sqrt{1 + \left(\frac{2l}{d}\right)^2}\right] + \frac{d}{2l} - \sqrt{1 + \left(\frac{d}{2l}\right)^2} + \mu_r \delta \right] \quad (3)$$

$$\delta = 0.25 \tanh\left(\frac{4d_s}{d}\right) \quad (3a)$$

$$d_s = \sqrt{\frac{\rho}{\pi f \mu_0 \mu_r}} \quad (3b)$$

$$L_4 = L_3 - \left(\frac{\mu_0 l}{2\pi}\right) \left[\ln \left[\frac{1}{a} + \sqrt{1 + \left(\frac{l}{a}\right)^2} \right] + \frac{a}{l} - \sqrt{1 + \left(\frac{a}{l}\right)^2} \right] \quad (4)$$

where l = wire length, d = wire diameter, μ_0 = permeability of free space ($4\pi \times 10^{-7}$ H/m), μ_r = relative permeability of the bond wire material, δ = skin depth factor, d_s = skin depth of the bond wire material, ρ = resistivity of the bond wire (2.5×10^{-8} Ω -m for gold), f = frequency, a = wire height. Equation (2) is a first order approximation. It represents the "free space" inductance of a straight wire positioned horizontally at an infinite distance above a conducting ground and is valid only up to UHF. Equation (3) accounts for the skin effect and equation (4) takes care of the ground plane effect on wave propagation assuming perfectly conducting ground.

Different wire shapes are considered in [3] by introducing a bonding angle parameter. According to [3], wire inductance is given by:

$$L_5 = 10 \int_0^{\frac{b}{2}} \ln \left[\frac{1}{d} \left[\sqrt{\left(\frac{d}{2} \operatorname{cosec} \beta\right)^2 - x^2} + c - \frac{d}{2} \cotan \beta \right] \right] dx \quad (5)$$

where b = distance between two bond connections, c = minimum average height of the pads, β = bonding angle, $0 < \beta < \pi/2$ and d = wire diameter, b , c , and d are all in inches.

In LIBRA, a commercial microwave circuit simulator [8], wires are modeled using series combination of inductance and resistance. No reference was found in LIBRA manual concerning the way these parameters are calculated, however, the only input parameters user has to provide are the wire diameter, length and metal resistivity. In the course of this work it was found that for long wires the inductance cannot be expressed as a function of just the wire length, rather both wire span and height are required.

As it will be shown later, the above models predict similar inductance values for relatively short wires, but differ significantly when long wires are considered.

2.2 TRANSMISSION LINE MODEL.

It was proposed [4] to model wires as transmission lines with characteristic impedances and effective dielectric constants. Based on a conformal mapping technique, line impedance, Z_0 , and effective dielectric constant, ϵ_{eff} , were found as:

$$Z_0 = 60 \cosh^{-1} \left[\frac{1 - \frac{1}{\left[\left(\frac{4(a+c)}{d} \right)^2 - 1 \right]^2}}{4} + \frac{1}{\left[\frac{8(a+c)}{d} - \frac{d}{2(a+c)} \right]} \right] \quad (6a)$$

$$\epsilon_{eff} = \frac{\ln \left[\frac{4(a+c)}{d} \right]}{\ln \left[\frac{4a}{d} + \frac{4c}{d\epsilon_r} \right]} \quad (6b)$$

where d = wire diameter, a = wire height, c = substrate thickness and ϵ_r = relative dielectric constant of the substrate. This model assumes straight transmission line suspended above the substrate. However, real-life wires are bent at either end and from this approach it is not clear how to account for different wire geometries, in particular, wire lengths. It will be shown later that the transmission line length is not exactly equal to the actual wire length. Therefore, the effective transmission line length parameter should be introduced.

2.3 WIRE RESISTANCE AND PAD CAPACITANCE.

Bonding pad capacitance and wire series resistance, shown in Figure 1, play only secondary role in bond wire performance. Bond wire capacitance could also be included in the LRC model, but it is even less important. It's value is usually less than 5% of the bond pad capacitance. Adding more parameters to the model will result in better fit with experimental data but the parameter values may not be physically meaningful.

Pad capacitance could be estimated using a simple parallel plate capacitor model, however fringing capacitance should be properly accounted for. A phenomenological formula for the pad capacitance was derived in [5]:

$$C_{\text{pad}} = 1.3 \frac{\epsilon_0 \epsilon_r P}{A} + 0.92 \frac{\epsilon_0 \epsilon_r A}{\log(10^4 H)} \quad (7)$$

where A = pad area and P = pad perimeter. However, this expression is valid for GaAs substrates only. In this work the metal pads were placed on top of the dielectric with $\epsilon_r = 140$. Because relative dielectric constant of the substrate was so high, the simple parallel plate capacitor model was used with a high degree of accuracy to set an initial pad capacitance value for the S-parameter optimization (see Chapter 3 for details). An alternative way to model large pad capacitors especially when multiple wire connections are considered is to use the analytical multi-port capacitor model [6]. This model, developed using second kind Green's functions and

based on the planar circuits theory, gives the same result as full-wave 2.5-dimensional numerical simulator only at a much higher speed.

As mentioned in [1], a common way to calculate the wire resistance is to use the following formula that accounts for the skin effect:

$$R_s = \frac{4l\rho}{\pi d^2} \left(0.25 \frac{d}{d_s} + 0.27 \right) \quad (8)$$

For 1 mil diameter Au wires considered in this work, series resistance per unit wire length is defined as follows:

$$\frac{R_s}{l} = 0.05(0.27 + 0.03\sqrt{f}) \quad (9)$$

where l is in millimeters and f is in GHz. Figure 5 shows the R_s/l dependence on frequency. As expected, at higher frequencies the wire series resistance increases, because the current that passes the wire is more crowded near the metal surface due to skin effect, therefore making wire cross-section effectively smaller.

Chapter 3

Proposed model extraction and verification

In this work, as first reported in [6] and in [12], bond wire modeling is based on results of numerical electromagnetic simulation performed using a commercial full-wave 2.5-dimensional software EM [7]. The present modeling scheme is summarized in Figure 6. After 3-dimensional wire geometry is entered into EM, a simulation is performed which yields two-port S-parameters. Lumped and distributed model parameters are then extracted from the simulated S-parameters using LIBRA [8]. LIBRA is invoked as a simulator within a schematic entry microwave circuit design package ACADEMY [9].

To validate the EM simulation, microwave S-parameters were measured from a wire with $a = 0.65$ mm and $b = 1.30$ mm. The transmission (S_{21}) and reflection (S_{11}) coefficients measured were compared to those calculated from the LRC model (Equation (4)) and to the result of EM simulation. As shown in Figures 7 and 8, EM simulation agrees better with the measurement than the LRC model.

The wire was bonded onto a coplanar microstrip structure suitable for on-wafer S-parameter measurements, as shown in Figure 9. Mech-EI model 209 tool was used to perform wire bonding. The equipment used for S-parameter measurements includes HP8510-B network analyzer in conjunction with two Cascade LIPH-305K-100 on-wafer probes mounted on an Alessi REL-3200 probe station. The equipment was controlled by ANACAT [10], that runs on a personal computer. Calibration of the system was done by moving the reference planes to the probe tips using an Open-Short-Load-Through procedure. A Tektronix CAL 96 sapphire calibration wafer with the corresponding coplanar patterns on it was used to calibrate the system up to 33.2 GHz.

Chapter 4

Results and Discussion

Based on the previously described scheme, lumped and distributed wire model parameters were extracted. The bond wires considered were 1 mil in diameter with wire height ranging from 0.25 to 1.5 mm and wire span from 1 to 4 mm. The wires were bonded to metal pads ($75\ \mu\text{m}$ by $75\ \mu\text{m}$) located on top of a substrate of relative dielectric constant of 140 and $140\ \mu\text{m}$ thick. The dependence of the wire inductance and effective transmission line length on wire span and height was studied and empirical formulas for both parameters were derived. The extracted wire inductances were found to be smaller than those predicted by the existing models. The wire-to-pad discontinuity was not modeled separately because metal spot size strongly depends on bonding conditions and on the ultrasonic power delivered to the bonding tip in particular making accurate modeling impossible.

4.1 LRC MODELING RESULTS.

The extracted bond wire equivalent circuit parameter values for the LRC model and optimization errors are summarized in Table 1. The wire inductance could be expressed as $L(\text{nH}) = -0.15 + 0.46b + 0.69a$, where b and a are in mm. The least squares fitting result is shown in Figure 10. It was found that a similar expression can not be written for round wires using only a total wire length ($2l = \pi b$). An attempt of such fitting is shown in Figure 11. Figure 12 shows that extracted wire inductance values were lower than any existing formula would predict. The lumped elements model accurately predicts performance of relatively short ($l \leq 2$ mm) wires up to about 16 GHz. The typical S_{11} and S_{21} fitting obtained for wires with $a = 0.5$ mm, $b = 1$ mm and $a = 0.9$ mm, $b = 2$ mm is shown in Figures 13 and 14. However, at higher frequencies and especially for long bond wires the LRC model is inaccurate. As shown in Figure 15, long bond wires have a peak transmission near millimeter frequencies. This important feature in principle cannot be predicted by the LRC model and is a characteristic of a transmission line.

4.2 TRANSMISSION LINE MODELING RESULTS.

Using the approach described in Section 3, distributed model parameters were extracted. The model parameter values and optimization errors are summarized in Table 2. The distributed model accuracy is an order of magnitude higher than that of the lumped model. The difference is especially pronounced at higher frequencies and for longer wires. Figure 16 compares the EM simulation result for a wire 0.9 mm high and 4 mm in span with the extracted lumped and distributed models. The wire transmission property is accurately predicted by the transmission line model up to 33.2 GHz, whereas LRC model extracted for 0.2 to 33.2 GHz frequency range departs from the simulated data above 10 GHz. Clearly, the distributed model should be used to predict wire behavior at high frequencies. Figure 17 shows the dependence of effective transmission line length on wire span and height fitted into a simple empirical expression. The obtained effective dielectric constant values are plotted in Figure 18. As expected, ϵ_{eff} decreases with increasing a and b as the effect of the dielectric substrate diminishes.

Both LRC and transmission line models can be used in LIBRA [8], as user-defined elements. While the canned-in LIBRA wire model requires wire diameter, length and metal resistivity as inputs, LRC and transmission line models would ask a user to enter wire span and height. There has not been found a fitting expression for ϵ_{eff} , therefore it has to be initially entered using Figure 18 as reference and then

optimized. An example netlist line that specifies the user-defined wire model in LIBRA will look as follows:

LRCWire [node 1] [node 2] *a* = [wire span] *b* = [wire height]

4.3 EFFECT OF NON-SYMMETRICAL SHAPE.

It is typical for present bonding techniques to yield wires with a non-symmetrical shape. The effect of non-symmetry on wire transmission was also studied. The S-parameters for three types of wires with same $H=0.5$ mm and $S=1$ mm but different symmetry (Figure 19) were simulated and compared. As shown in Figures 20 and 21, the transmission and reflection coefficients for all three cases were found to be almost identical. Henceforth, all the wires can be treated in the simulations as having symmetrical shape.

Chapter 5

Conclusions

Accurate and efficient lumped and distributed models have been developed for long bond wires. Below 16 GHz and for bond wires shorter than 2 mm, a simple LRC model is used in which the inductance is expressed in terms of wire span and height rather than total wire length. Above 16 GHz a transmission line model is required. Non-symmetry plays negligible role on the characteristics of short bond wires. Both models are conveniently incorporated in a commercial microwave integrated circuit simulator, making simulations simple and efficient.

Chapter 6

Future work

Having analyzed specifically 1 mil diameter bond wire structures, it is natural to extend the range of studies to wires with different diameters. Other typically used diameters are 0.5, 0.7 and 2 mils. Gold ribbons which are widely used in microwave packages could also be a subject of research. It is also important to extend the distributed model to include wires placed on top of the substrates with other than 140 relative dielectric constant. Unfortunately, the whole approach is not applicable to characterization of wires connecting different substrates, because EM is not capable of analyzing multiple substrate structures. Finally, more direct experimental verification of the developed models requires special set of coplanar patterns designed for on-wafer S parameter measurements of wires with different spans.

BIBLIOGRAPHY

- [1] F.E. Terman, *Radio Engineers' Handbook*, McGraw Hill, 1943.
- [2] S.L. March, "Simple equations characterize bond wires", *Microwave & RF*, pp 105-110, Nov. 1991.
- [3] J.P. Mondal, "Octagonal spiral inductor measurement and modeling for MMIC applications", *Int. J. Electronics*, vol. 68, no. 1, pp. 113-125, 1990.
- [4] R.H. Caverly, "Characteristic impedance of integrated circuit bond wires", *IEEE Trans. Microwave Theory Tech.*, vol. MTT-34, no. 9, pp. 982-984, Sept. 1986.
- [5] A. Higashisaka and F. Hasegawa, "Estimation of fringing capacitance of electrodes on S.I. GaAs substrate", *Electronic Lett.*, vol. 16, pp. 411-412, 1980.
- [6] Y.A. Tkachenko, C.J. Wei and J.C.M. Hwang, "Models for long bond wires and large multi-port capacitors", *Proc. IEEE Princeton Section Sarnoff Symposium*, 1993.
- [7] Sonnet: emtm, xgeomtm and emvutm version 2.3, 1989 by Sonnet Software Inc., USA.
- [8] EEsof: Libratm version 3.5, 1992 by EEsof, Inc., USA.
- [9] EEsof: ACADEMYtm version 3.5, 1992 by EEsof, Inc., USA.
- [10] EEsof: ANACATtm version 3.5, 1992 by EEsof, Inc., USA.
- [11] C.J. Wei, Y. Lan, Y.A. Tkachenko and J.C.M. Hwang, "A comprehensive nonlinear model for Class-AB high-power amplifiers", submitted to *IEEE GaAs Symp.*, Atlanta, Ga, 1993.
- [12] Y.A. Tkachenko, C.J. Wei and J.C.M. Hwang, "Models for long bond wires", submitted to *IEEE Microwave and Guided Wave Lett.*, 1993.

a , mm	b , mm	L , nH	R , m Ω	C , pF	Error %
0.26	1.00	0.50	133	0.47	0.15
	2.00	1.00	133	0.48	0.23
	3.20	1.55	140	0.50	0.30
	4.00	1.80	148	0.53	1.10
0.50	1.00	0.63	133	0.48	0.13
	2.00	1.13	190	0.49	0.17
	3.20	1.71	199	0.50	0.28
	4.00	2.08	195	0.51	0.59
0.90	1.00	0.90	129	0.48	0.14
	2.00	1.40	210	0.49	0.20
	3.20	1.97	218	0.51	0.42
	4.00	2.30	195	0.52	2.23
1.50	1.00	1.33	129	0.49	0.14
	2.00	1.86	198	0.49	3.67

Table 1. Extracted LRC model parameters.

a , mm	b , mm	L_{eff} , mm	C , pF	ϵ_{eff}	Error, %
0.26	1.00	0.86	0.44	10.63	0.10
	2.00	1.72	0.45	5.55	0.13
	3.20	2.69	0.46	3.22	0.13
	4.00	3.34	0.47	2.31	0.11
0.50	1.00	1.06	0.46	5.89	0.11
	2.00	1.94	0.46	4.14	0.10
	3.20	2.97	0.46	2.71	0.01
	4.00	3.62	0.47	1.96	0.01
0.90	1.00	1.52	0.46	3.75	0.11
	2.00	2.41	0.46	3.40	0.01
	3.20	3.42	0.47	2.13	0.01
	4.00	3.80	0.48	2.17	0.10
1.50	1.00	2.27	0.46	2.46	0.31
	2000	3.16	0.46	2.18	2.91
	3200	4.00	0.48	1.01	8.05

Table 2. Extracted transmission line model parameters.

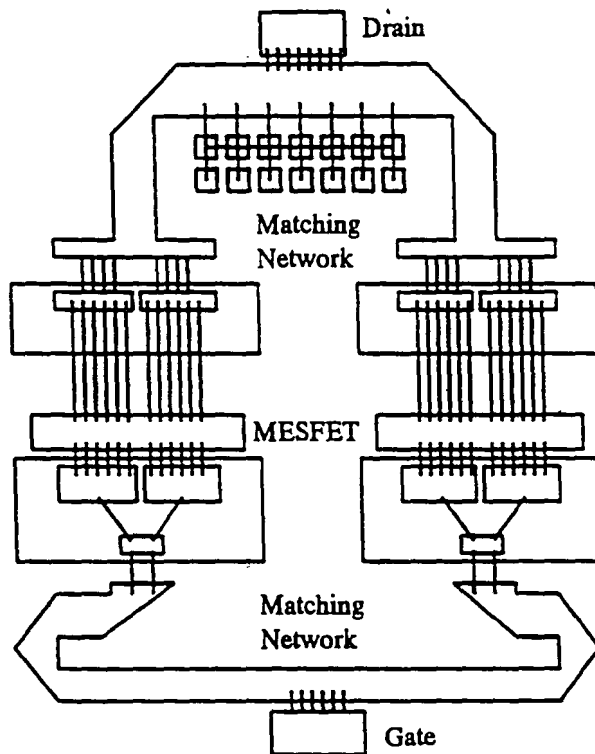


Figure 1. Schematic of a 10 W C-band MESFET amplifier.

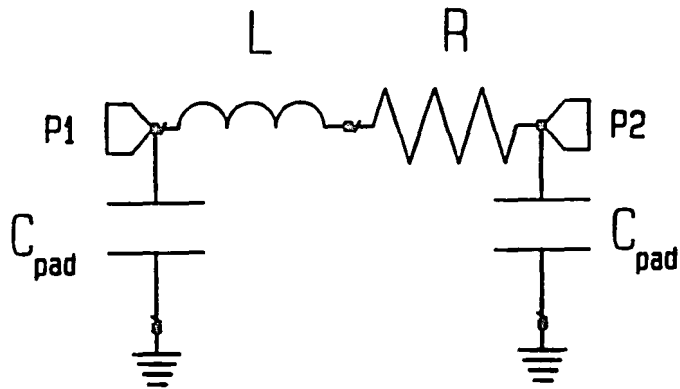


Figure 2. Lumped LRC model of a bond wire.

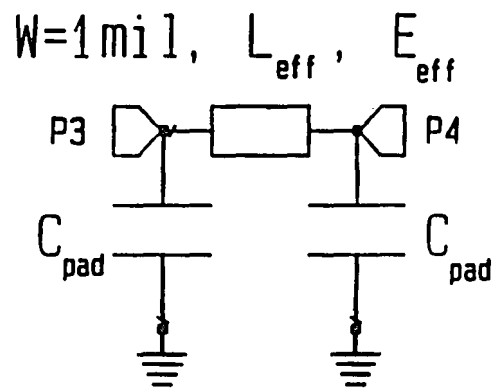


Figure 3. Transmission line model of a bond wire.

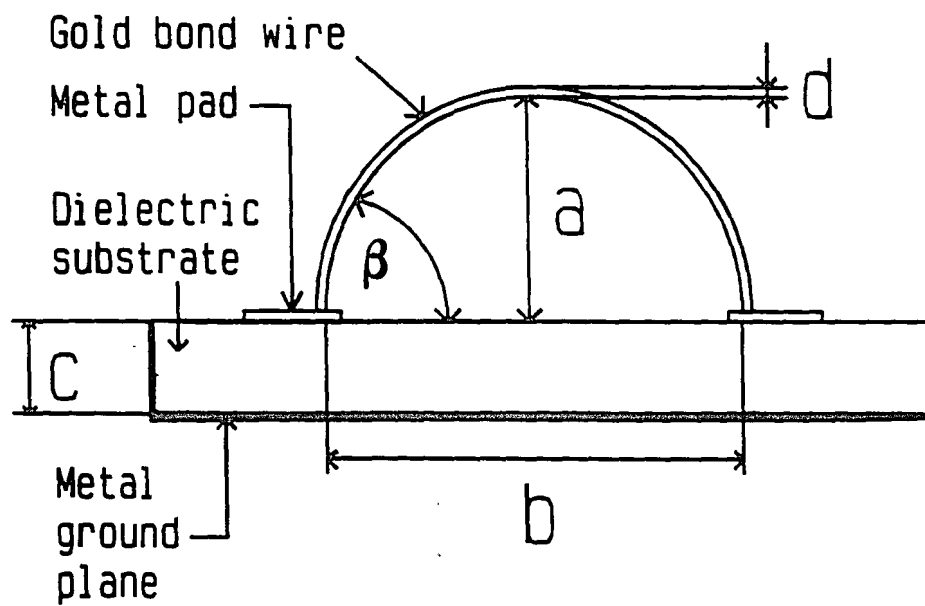


Figure 4. Schematic of a bond wire structure.

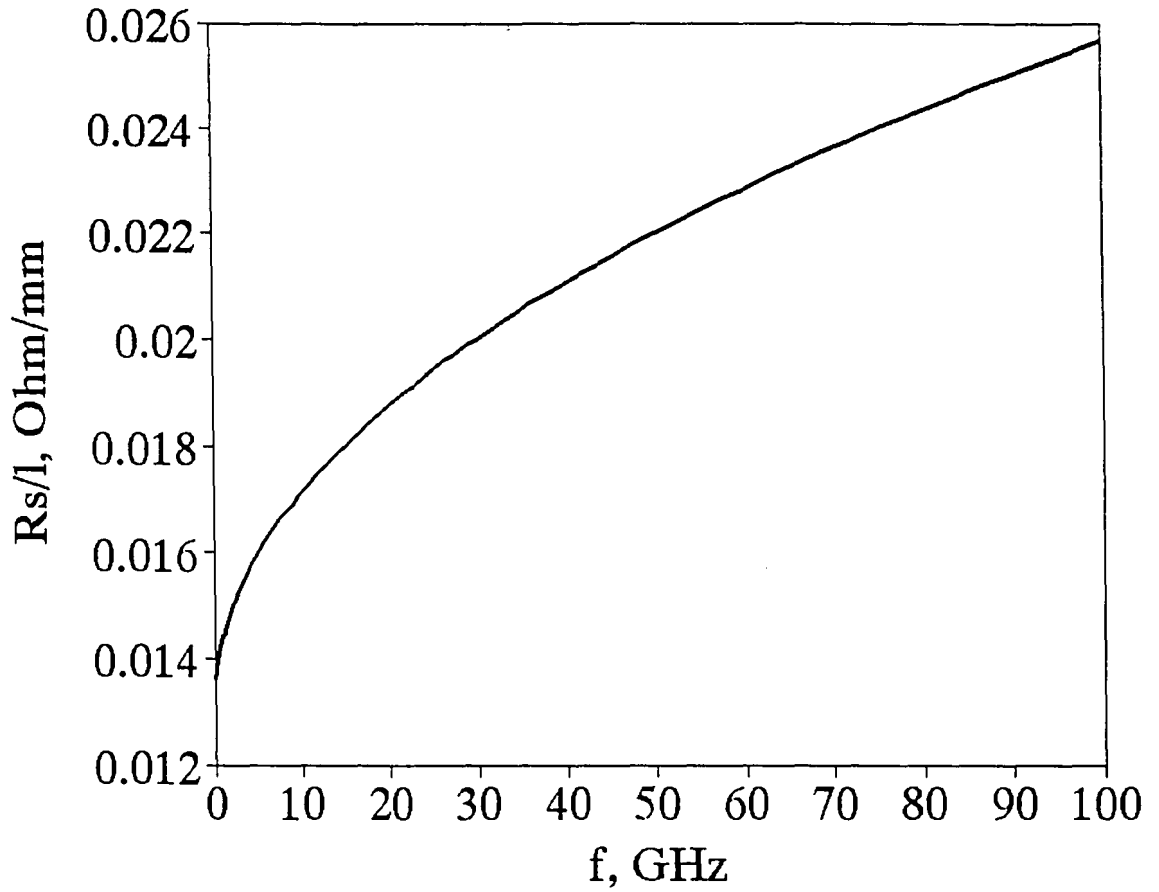


Figure 5. Per unit length series resistance of wires 25 μm in diameter.

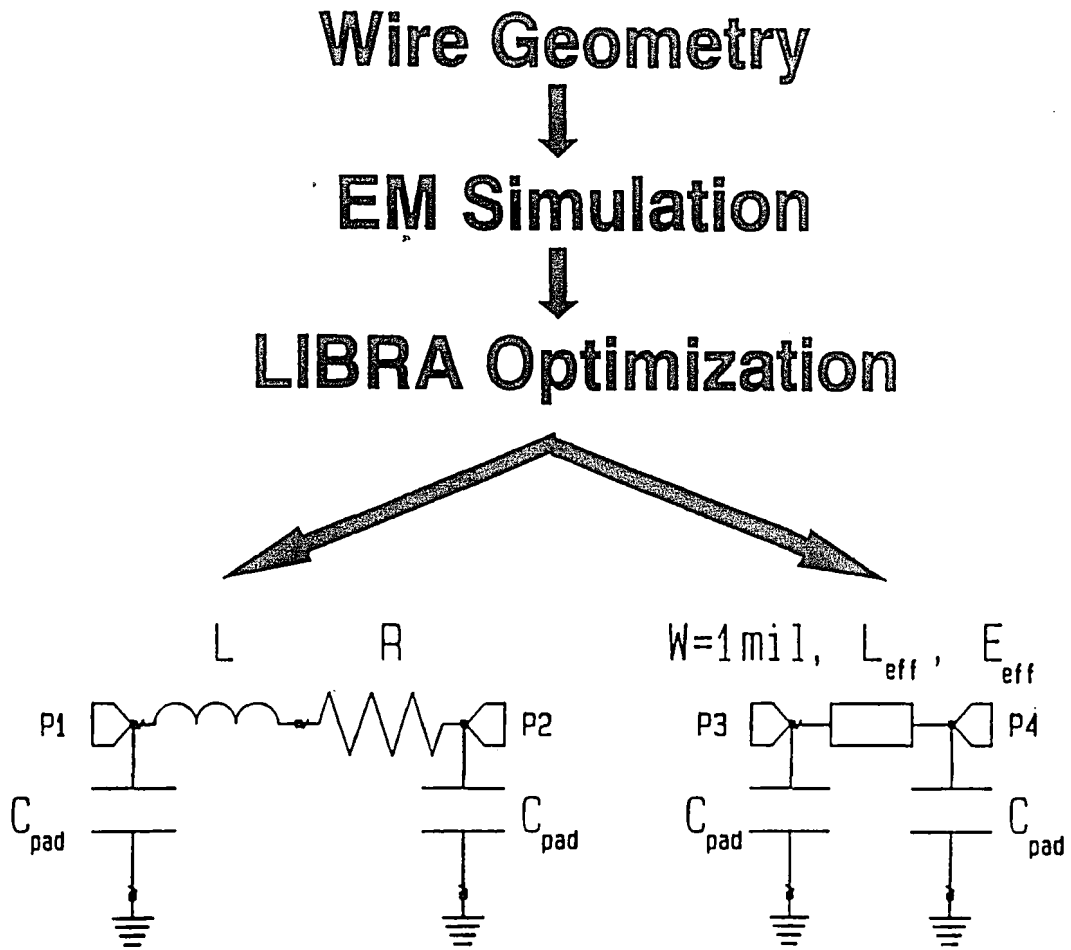


Figure 6. Proposed bond wire modeling scheme.

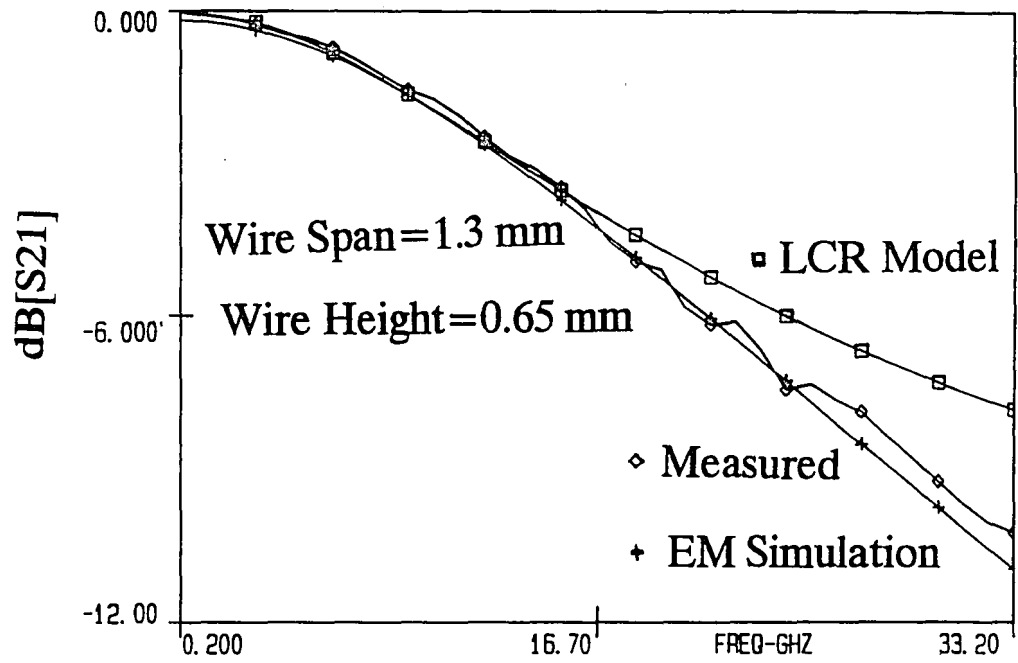


Figure 7. Modeled [2], em simulated and measured transmission coefficient S_{21} of a wire 0.65 mm high and 1.33 mm in span.

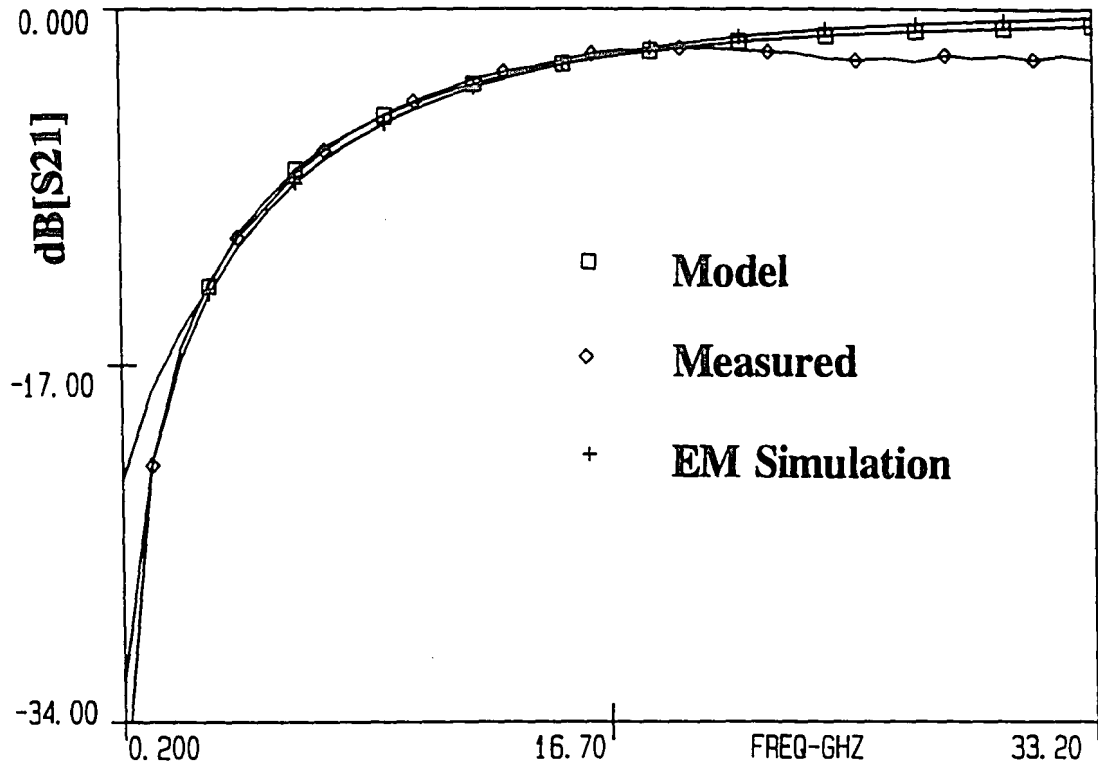


Figure 8. Modeled [2], em simulated and measured reflection coefficient S_{11} of a wire 0.65 mm high and 1.3 mm in span.

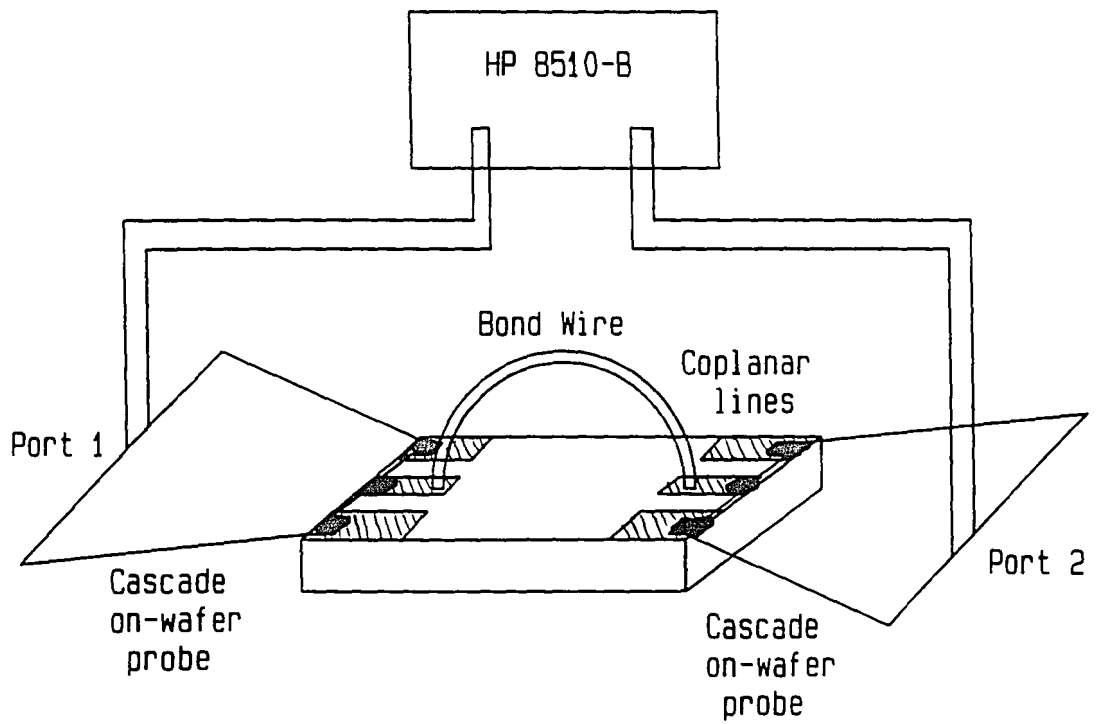


Figure 9. Bond wire measurement schematic.

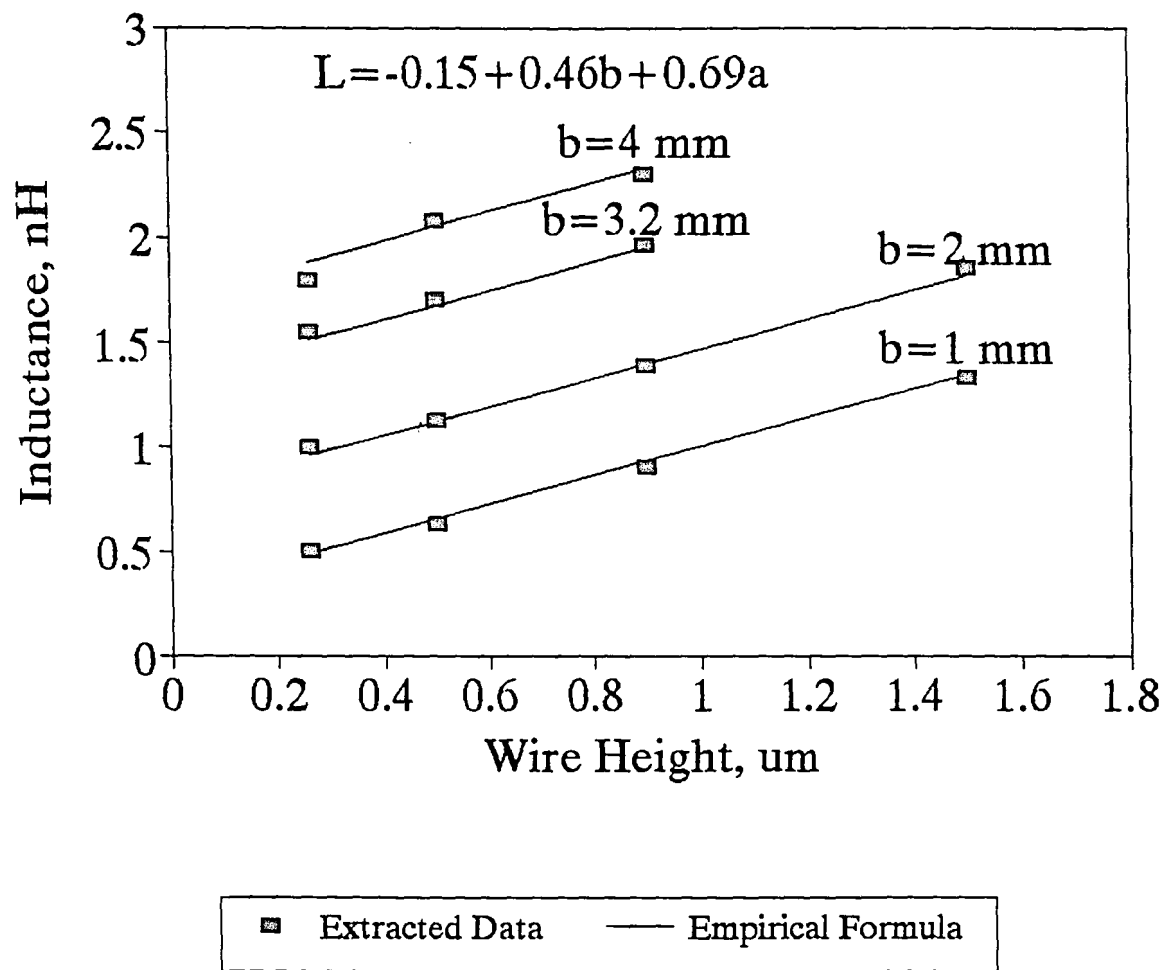


Figure 10. Extracted wire inductances as a function of wire span and height.

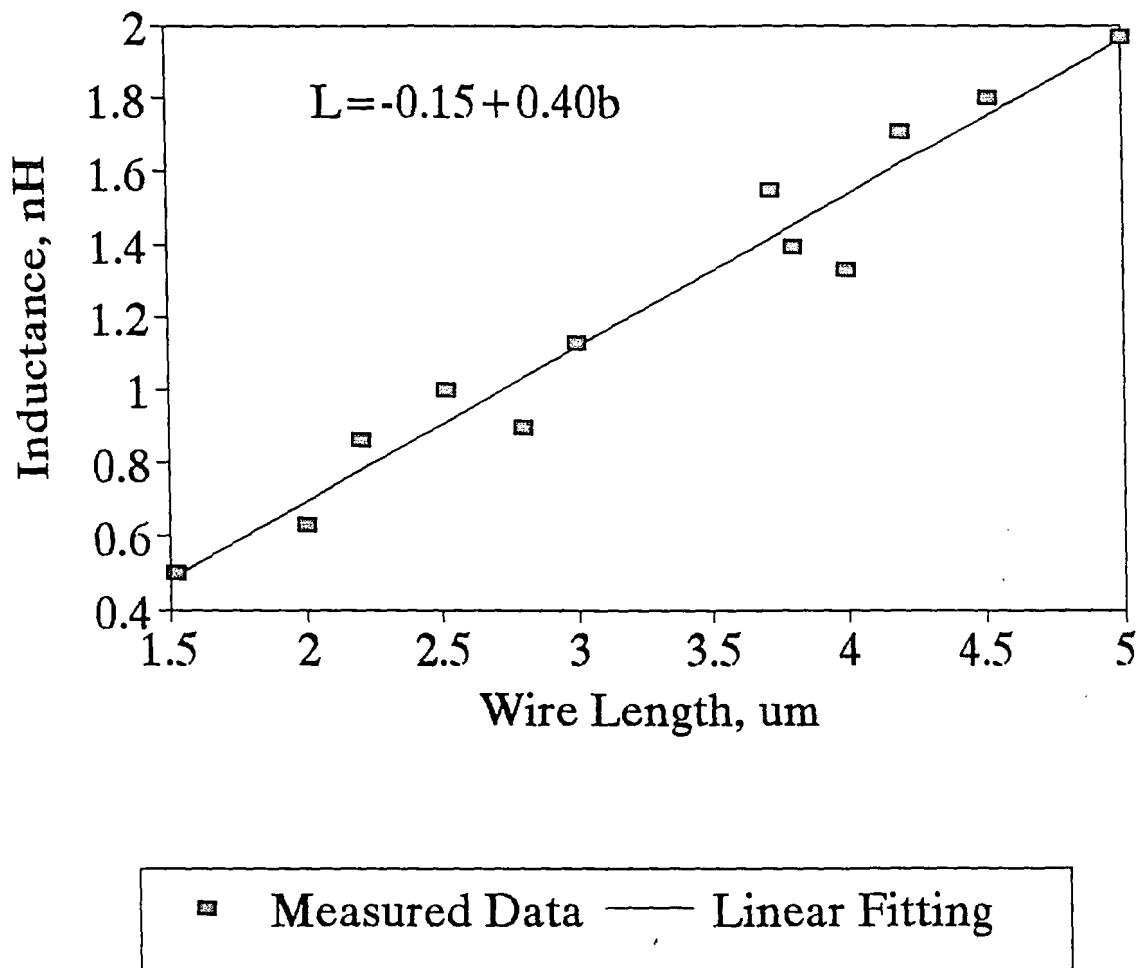


Figure 11. Extracted wire inductances as a function of wire length only.

Inductance Calculations

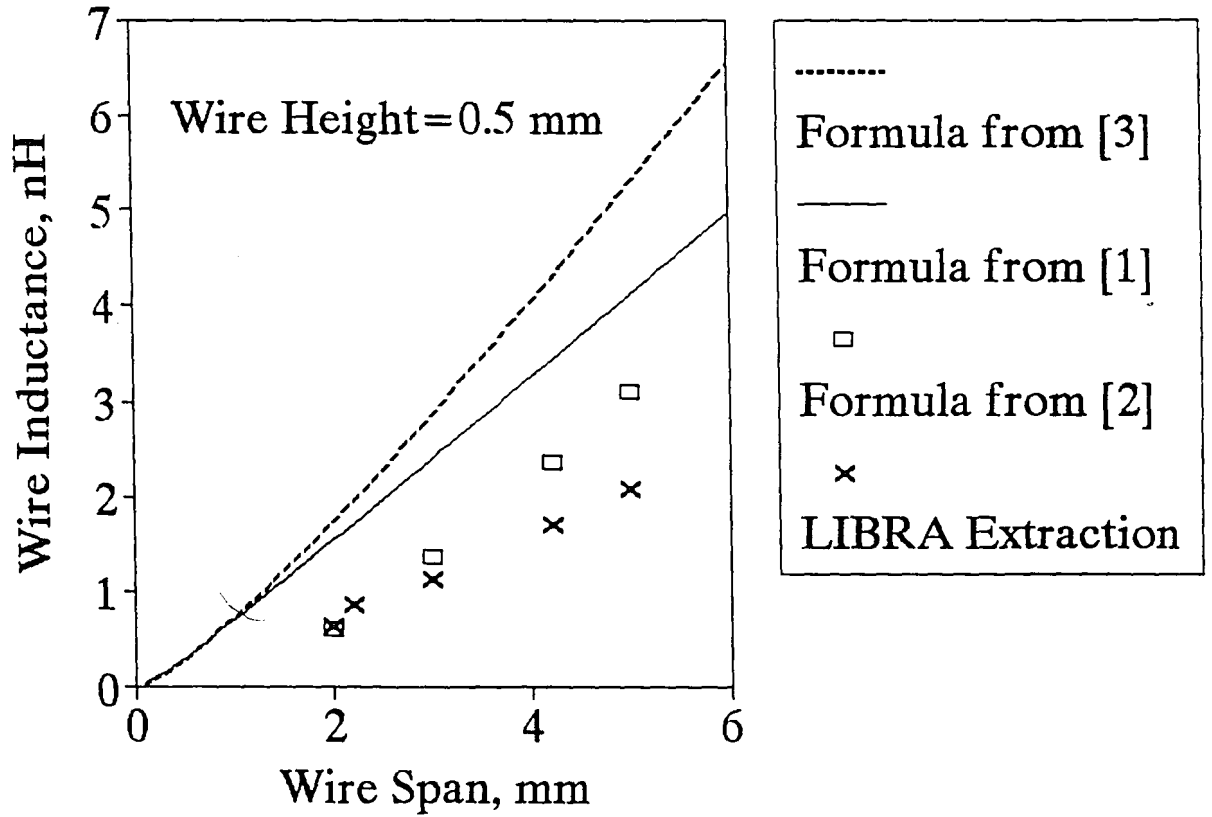


Figure 12. Wire inductance calculated according to [1], [2], [3] and extracted values.

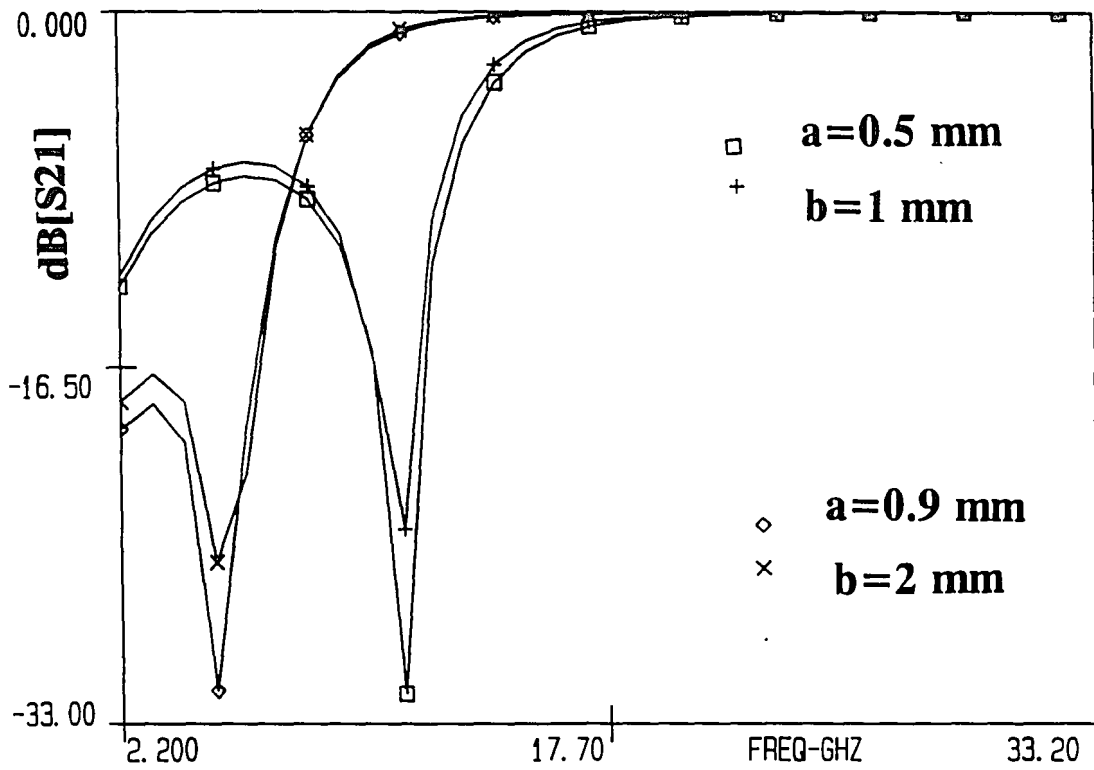


Figure 13. Em simulated and modeled reflection coefficient S_{11} of wires with $a = 0.5 \text{ mm}$, $b = 1 \text{ mm}$ and $a = 0.9 \text{ mm}$, $b = 2 \text{ mm}$.

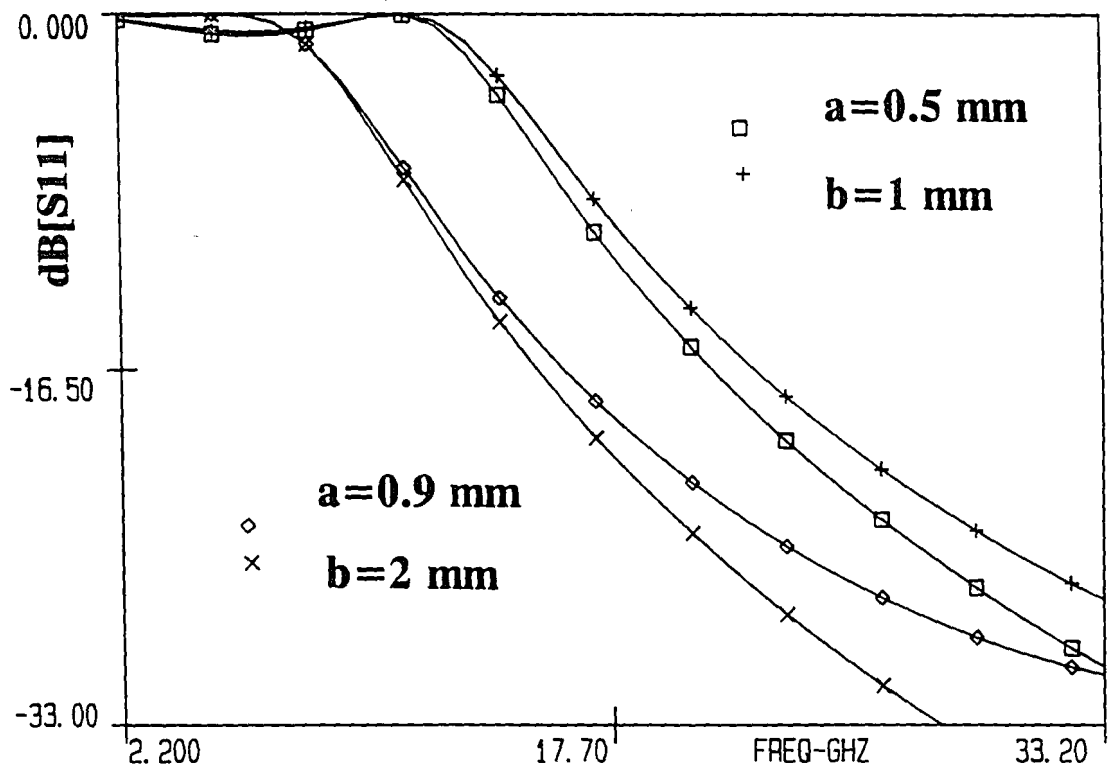


Figure 14. Em simulated and LRC modeled transmission coefficient S_{21} of wires with $a = 0.5$ mm, $b = 1$ mm and $a = 0.9$ mm, $b = 2$ mm.

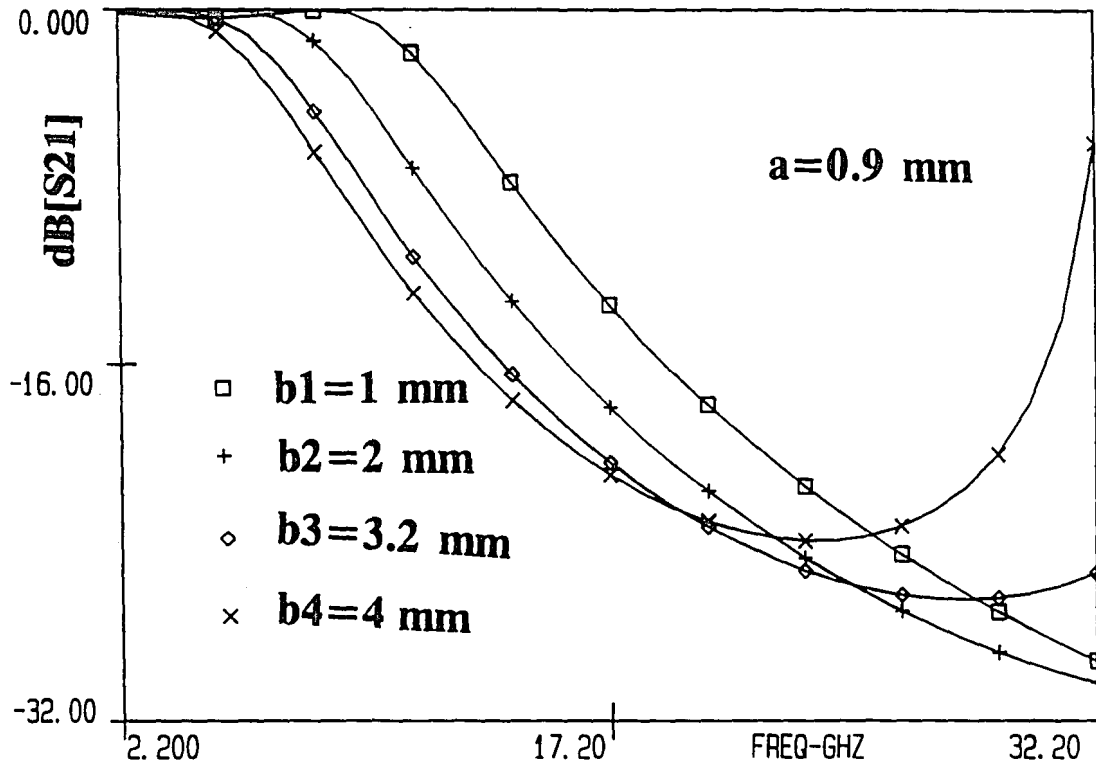


Figure 15. Simulated transmission coefficient S_{21} of wires 0.9 mm high and 1, 2, 3.2 and 4 mm in span.

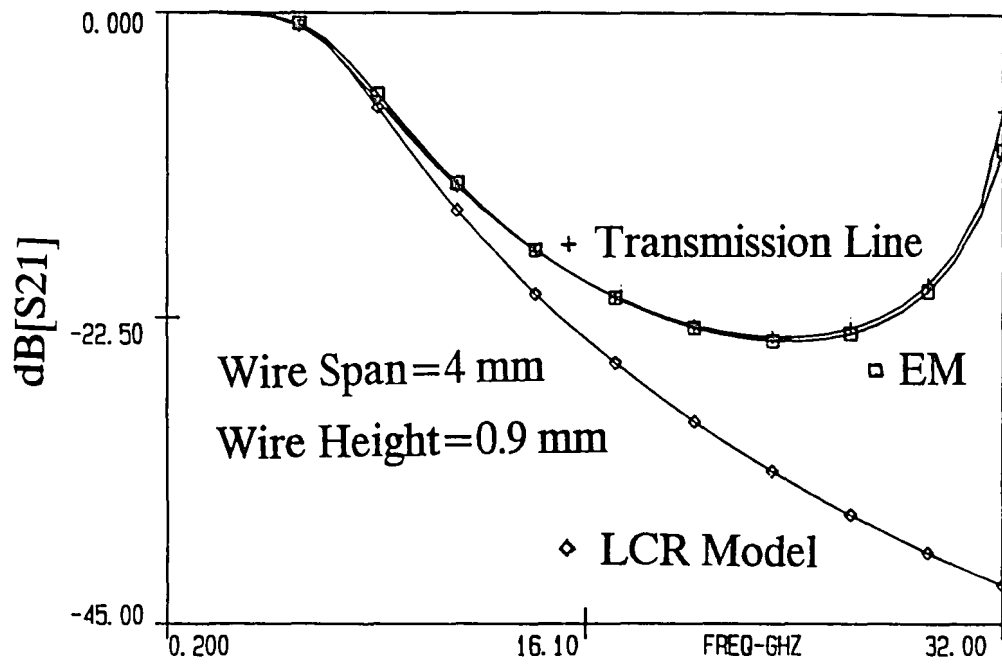


Figure 16. Transmission coefficient S_{21} of a wire 0.9 mm high and 4 mm in span predicted by em simulation and LRC and transmission line models.

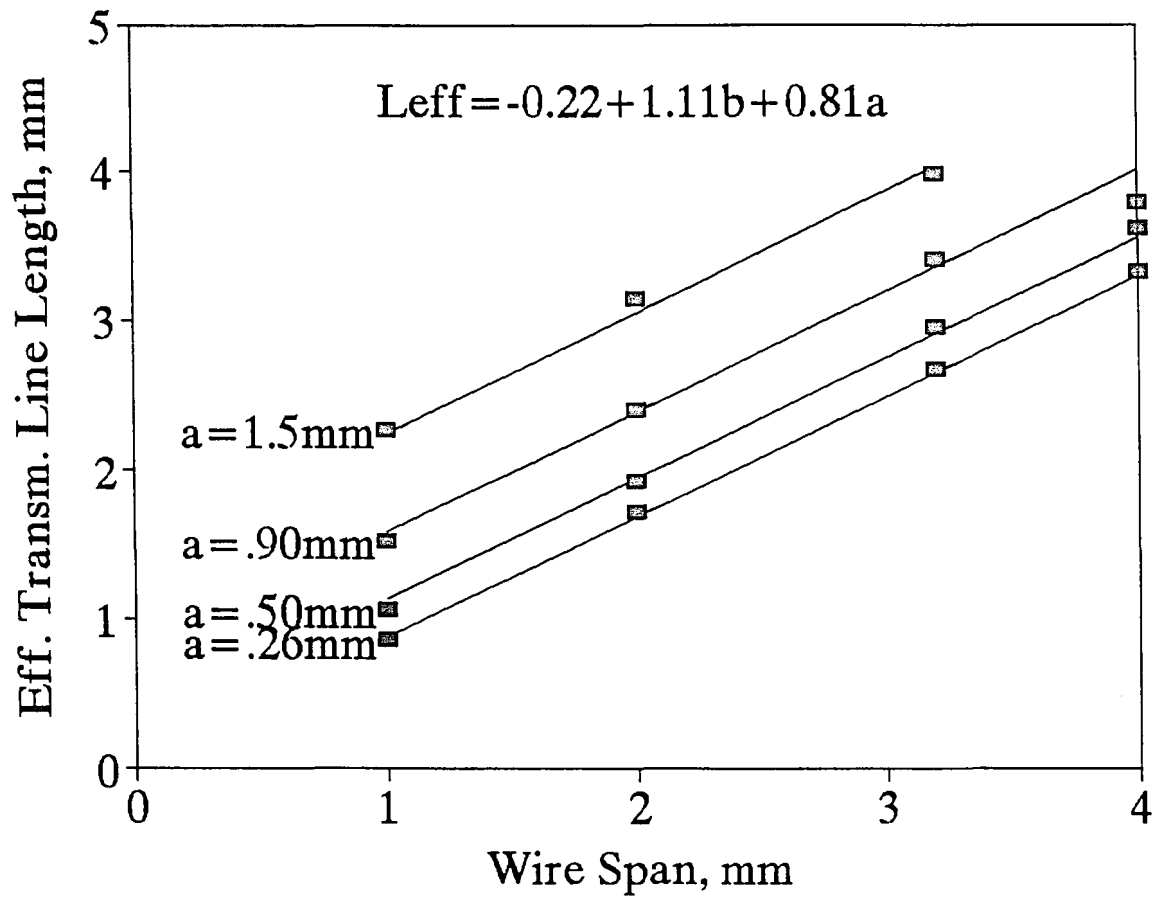


Figure 17. Extracted effective transmission line lengths.

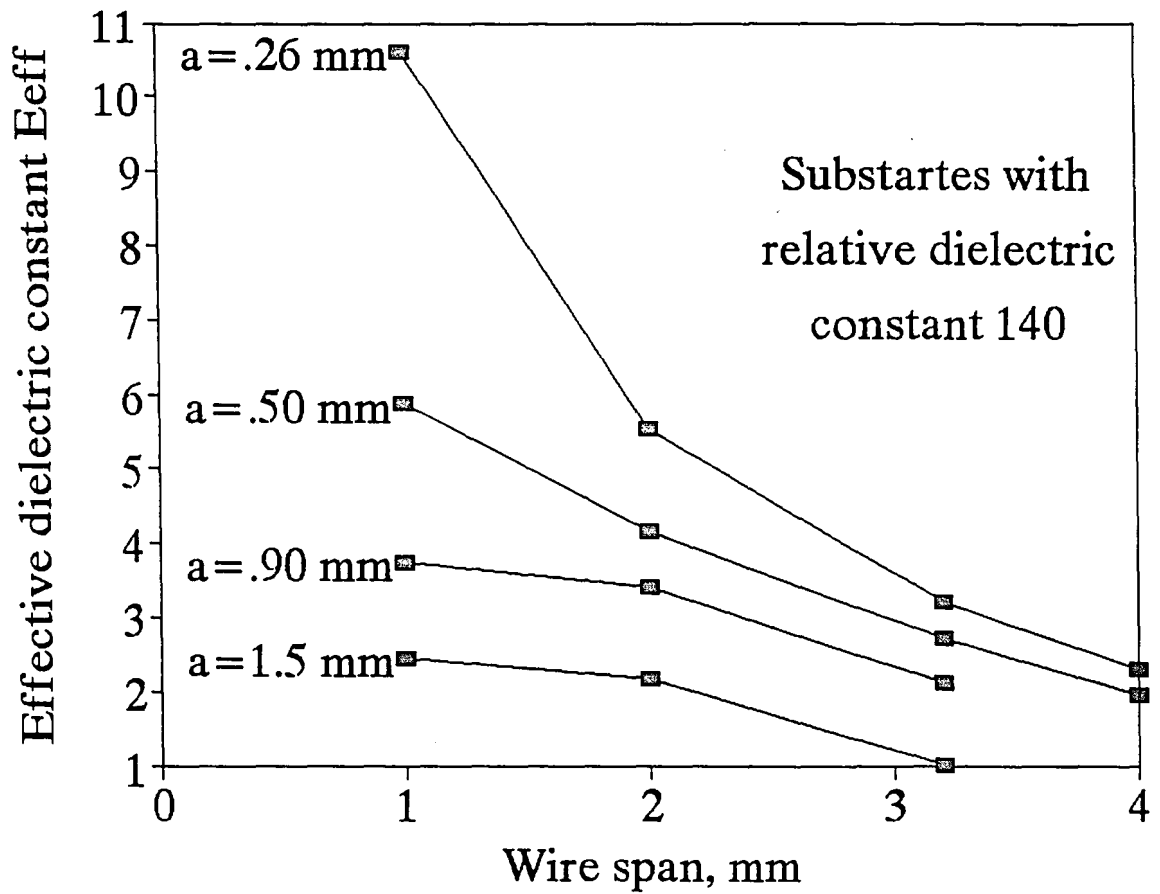


Figure 18. Extracted effective dielectric constants.

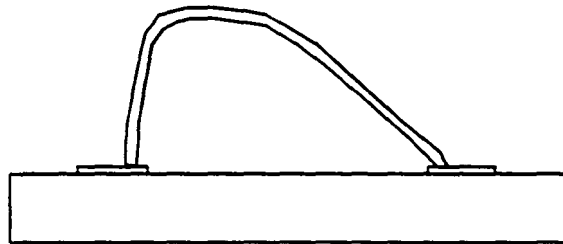
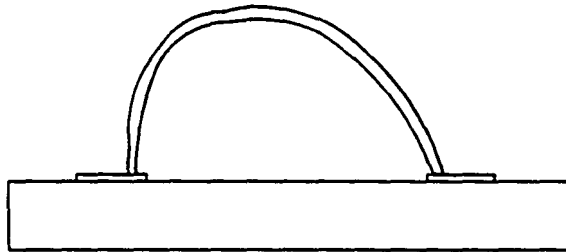
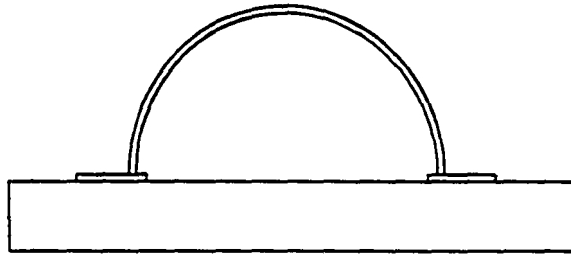


Figure 19. Symmetrical and non-symmetrical wire geometries used for simulation.

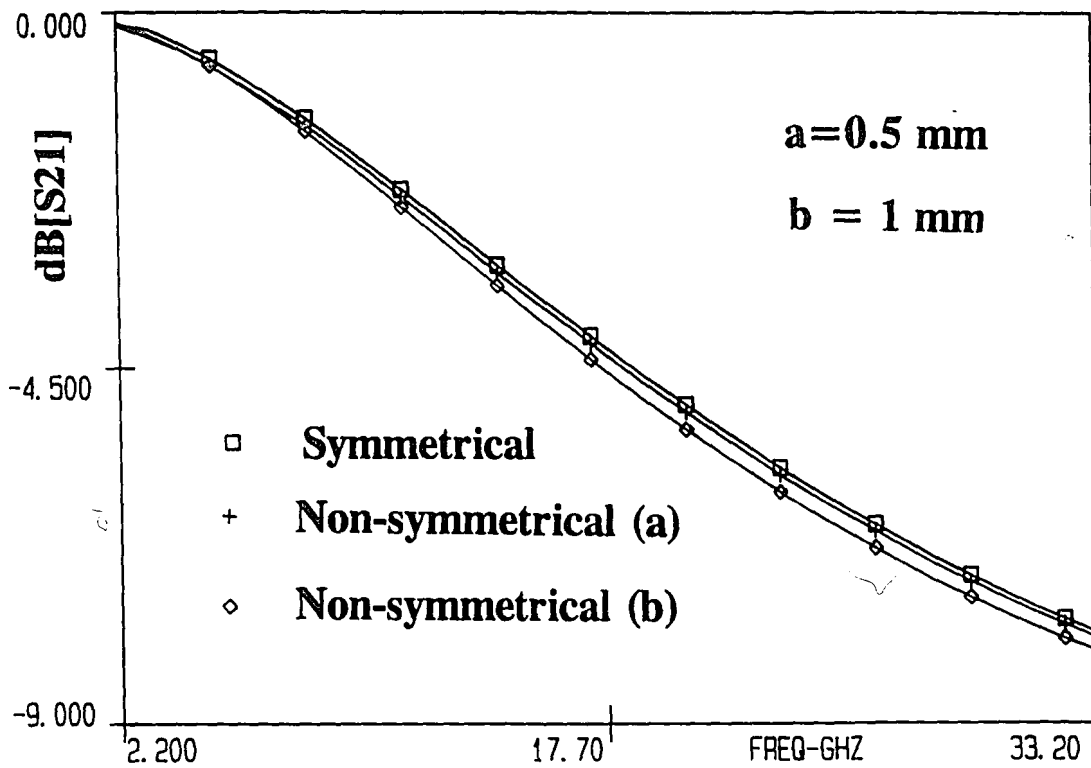


Figure 20. Em simulated transmission coefficient S_{21} of symmetrical and non-symmetrical wires 0.5 mm high and 1 mm in span.

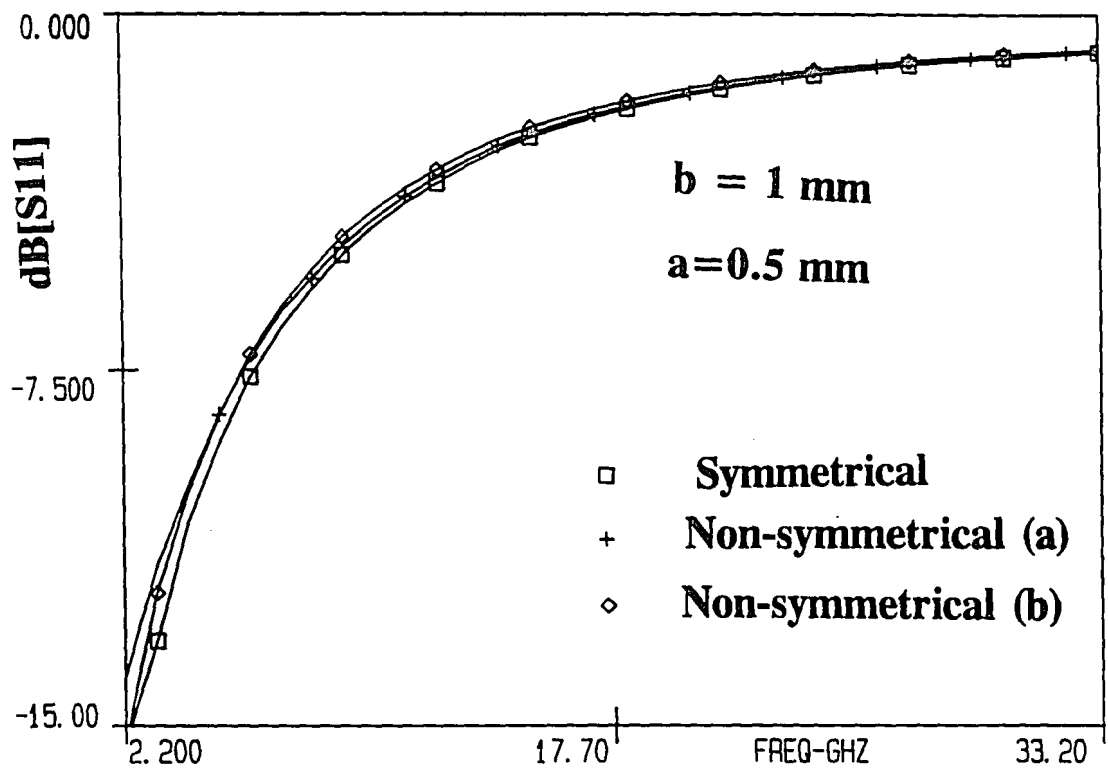


Figure 21. Em simulated reflection coefficient S_{11} of symmetrical and non-symmetrical wires 0.5 mm high and 1 mm in span.

VITA

Yevgeniy A. Tkachenko was born in Kiev, Ukraine on May 22, 1968. He was educated at Kiev Polytechnical Institute and at Lehigh University. After attending Lehigh University in 1990, Mr. Tkachenko graduated with a Bachelor of Science degree in Electrical Engineering in June 1991. Since 1991 he worked in the area of microwave devices and integrated circuits characterization and modeling at the Compound Semiconductor Technology Laboratory.

Publications:

1. "Models for long bond wires and multi-port capacitors", *Proc. IEEE Princeton Section Sarnoff Symposium*, 1993, with C.J. Wei and J.C.M. Hwang.
2. "Non-invasive waveform probing for nonlinear network analysis", *IEEE MTT-S International Microwave Symposium Digest*, Atlanta, Ga, 1993, with C.J. Wei and J.C.M. Hwang.
3. "Comprehensive modeling of class-AB high-power amplifiers", submitted to *IEEE GaAs IC Symposium*, San Jose, 1993, with C.J. Wei, Y. Lan and J.C.M. Hwang.
4. "Degradation mechanisms of power MESFET's", submitted to *IEEE GaAs IC Symp. Reliability Session*, San Jose, 1993, with C.J. Wei, Y. Lan, D.S. Whitefield and J.C.M. Hwang.
5. "Models for long bond wires and multi-port capacitors", submitted to *IEEE Guided Wave Letters*, 1993.
6. "Waveform analysis of power slump of GaAs MESFET'S", to be published elsewhere, 1993, with C.J. Wei, Y. Lan and J.C.M. Hwang.

Presentations:

"Models for long bond wires and large multi-port capacitors", presented at IEEE Princeton Section Sarnoff Symposium, Princeton, NJ, 1993.

Societies and Awards:

Mr. Tkachenko is a member of Phi Beta Delta honorary society for international scholars, IEEE Electron Device, Power Engineering and Microwave Theory and Techniques Societies. He has been awarded Sherman Fairchild Scholarship in 1992 and 1993.

END

OF

TITLE